Video Article

# A Rat Model of Radiation Vasculitis for Mesenchymal Stem Cell-based Therapy

Xuan Tao*[1], Mingyang Sun*[1], Rongchao Ying[2], Wenjie Su[2], Wei Wei[1], Xiaohu Meng[1]

[1]Division of General Surgery, Second Affiliated Hospital of Nanjing Medical University

[2]Division of General Surgery, Hangzhou First People's Hospital Affiliated to Nanjing Medical University

*These authors contributed equally

Correspondence to: Wei Wei at kevinwei@njmu.edu.cn, Xiaohu Meng at 1193970654@qq.com

URL: https://www.jove.com/video/58899
DOI: doi:10.3791/58899

Keywords: Radiation, vascular injury, vasculitis, rat, aortatransplantation, intimal hyperplasia, fibrosis

Date Published: 10/5/2018

Citation: Tao, X., Sun, M., Ying, R., Su, W., Wei, W., Meng, X. A Rat Model of Radiation Vasculitis for Mesenchymal Stem Cell-based Therapy. *J. Vis. Exp.* (), e58899, doi:10.3791/58899 (2018).

## Abstract

Radiation vasculitis is one of the most common detrimental effects of radiotherapy for malignant tumors. This is developed at the vasculature of adjacent organs. Animal experiments have shown that the transplantation of mesenchymal stem cells (MSCs) restores vascular function after irradiation. However, the population of MSCs migrating to irradiated vessels is too low in the conventional models, which makes an assessment of the therapeutic effect difficult. This is presumably because circulating MSCs are dispersed in adjacent tissues that are being irradiated simultaneously. Based on this assumption, a specific rat model, namely RT (radiation) plus TX (transplantation), was established to promote MSC homing by sequestering irradiated vessels. In this model, a 1.5 cm-long segment of rat abdominal aorta was irradiated by a 160 kV X-ray at a single dose of 35 Gy before being procured and grafted to the healthy counterpart. F344 inbred rats served as both donors and recipients to exclude the possibility of immune rejection. A beam-limiting device was used to confine the X-ray beam to a 3 x 3 cm square-shaped field covering the central abdominal region. The abdominal viscera, especially the small bowel and colon, were protected from irradiation by being pushed off the central abdominal cavity. Typical radiation-induced vasculopathy was present on the 90th day after irradiation. The recruitment of intravenously injected MSCs to the irradiated aorta was significantly improved by using the RT-plus-TX model as compared to the model with irradiation only. Generally, the RT-plus-TX model promotes MSC recruitment to the irradiated aorta by separating the irradiated vascular segment from the adjacent tissue. Thus, the model is preferred in the study of MSC-based therapy for radiation vasculitis when the evaluation of MSC homing is demanding.

## Introduction

Radiotherapy is used to treat a variety of cancers, but the therapeutic index of radiotherapy is still limited by normal tissue injury in organs at risk. Vascular injury is the major cause of late radiation morbidity. Patients with head and neck tumors have a higher risk of developing dementia and cognitive dysfunction after radiotherapy[1,2]. Despite direct ionizing radiation injury to neurons and glial cells, brain blood circulation disorder resulting from vascular injury is an essential contributory factor[3,4]. The small bowel is very vulnerable to irradiation. Chronic radiation enteritis is initiated as early as 2 months after patients received abdominal/pelvic irradiation, progressing throughout the rest of their life[5]. This is characterized by progressive obliterative arteritis with submucosal fibrosis[5]. Typically, the irradiated vessels develop slowly toward vascular fibrosis with luminal stenosis, excessive extracellular matrix deposition in the media and adventitia, intimal hyperplasia, and thrombus formation[4]. The process has been replicated by rat models, in which radiation-induced vasculopathy is present 3 - 6 months after irradiation[6,7]. Many potential therapeutic strategies have been investigated in these models prior to their clinical use.

Stem cell therapy holds great promise for radiation-induced vascular injury. MSCs are multipotent stromal cells that can differentiate into a variety of mature cell types. Moreover, MSCs themselves secrete a broad spectrum of trophic factors that serve to structure regenerative microenvironments[8]. MSCs were first separated from bone marrow and later found in other mesenchyme tissue. Their ease of isolation and manipulation and their potential use for tissue regeneration are specifically what has made them so attractive[9]. A number of animal studies have demonstrated that MSCs restore vascular function by both intravascular injection and seeding of vascular graft[6,8,10,11,12]. Nevertheless, it has been rarely reported how many circulating MSCs exactly reach irradiated vessels after intravascular injection, presumably because the recruited cell number is fairly low. This is a practical problem in MSC-based therapy for radiation injury and other diseases as well[8]. In a sense, the scarcity of MSCs in irradiated vessels renders the assessment of therapeutic effect somewhat difficult, given that MSC recruitment is a prerequisite for effective cell-based therapy[13]. One possible explanation for the phenomenon is that transplanted MSCs are dispersed in adjacent tissues, which are inevitably irradiated but constitute a large compartment of MSC recruitment. In that case, the effort to localize radiation exposure probably enable MSCs to aggregate in irradiated vessels. The assumption is supported by a previous investigation of the quantitative and spatial distribution of infused MSCs after local irradiation. Total body irradiation-stimulated MSCs homed at a very low level to various tissues of the whole body with additional local irradiation resulted in significant MSC engraftment in the exposed area[14]. Inspired by the findings, this study introduces a rat model, namely RT plus TX, in which irradiated vessels are sequestered from adjacent tissue to promote MSC local recruitment.

## Protocol

All animal procedures were approved by the Committee of Animal Experiment Ethics at Nanjing Medical University (Nanjing, China).

## 1. Animal and Cell Lines

1. Use female F344 rats at 12 weeks of age for the surgical procedures in this protocol, like abdominal irradiation and aorta transplantation, and as the host for MSC transplantation. Raise the rats in a specific pathogen-free grade barrier facility with a 12/12 h light/dark cycle, the temperature at 18 - 22 °C, and the relative humidity at 40% - 60%. Feed the rats with standard pelleted food and water.
2. Include 48 rats in the study. Divide them evenly into six groups according to the treatment protocols (**Table 1**).
3. Use male F344 rat MSC cell lines for the cell transplant. Culture the cells in Dulbecco's modified Eagle's medium (DMEM) supplemented with 10% fetal bovine serum (FBS) at 37 °C with a humidified atmosphere of 5% $CO_2$ and 95% air.
   NOTE: MSC transplantation from male donors to female recipients enables cell tracing by the sex determination region on the Y chromosome (Sry).

## 2. Abdominal Irradiation

1. Inject the rat with 10% chloral hydrate solution at a single dose of 0.3 mL per 100 g body weight *via* the intraperitoneal route. Wait 5 min to assess the anesthetic depth using reflex testing.
2. Fix the rat in a supine position with its four legs stretched outward. Prep the abdominal skin by shaving its hair and disinfecting it with 70% ethanol (EtOH).
3. Make a 5 cm midline incision by using scissors to open the abdominal cavity. Pull out the small bowel and the colon by using saline-soaked cotton swabs, and leave them to the right of the abdominal cavity, beyond the field of irradiation. Place the small bowel and colon on a piece of gauze that is wetted with warm saline to keep them moist.
4. Transfer the rat to the chamber of a biological irradiator. Make sure the chamber door is securely closed throughout the irradiation process. There is no asphyxiation as the chamber is not airtight.
5. Irradiate the rat in a ventrodorsal direction with a 160 kV X-ray, operating at 25 mA and filtered with 0.3 mm of copper. Set the total irradiation dosage to 35 Gy at the rate of 1.75 Gy/min.
6. Localize the irradiation to a square-shaped field of 3 x 3 cm, encompassing the central abdominal region by using a beam-limiting device or a lead shield. Leave the viscera, especially the small bowel and the colon, off of the irradiation field, to avoid the devastating gastrointestinal adverse effect.
7. Open the chamber door and take the rat out after the completion of irradiation.
8. Push the small bowel and colon back into the abdominal cavity. Close the abdominal incision with a 3-0 **polyglactin** suture for the rats of the RT-only model, which are not subjected to aortic transplantation. Keep the rats in a warming blanket until they have recovered from the anesthesia.

## 3. Aorta Transplantation

1. Sterilize all surgical instruments before use.
2. Keep the rat fixed on the operating table after the completion of the irradiation. Note that an additional injection of 10% chloral hydrate solution is not necessary since the rat is still under anesthesia.
3. Push the small bowel and the colon aside to expose abdominal aorta by using a Colibri retractor. Perform most of the following surgical procedures under a stereomicroscope.
4. Carefully dissect the infrarenal aorta away from adjacent tissue by using two microtweezers. Ligate lumbar arteries branching from the aorta with 9-0 nylon sutures.
5. Procure a 1.5 cm-long aortic graft by cutting with microscissors when its blood flow is blocked by the ligation right below the infrarenal artery and at aortic bifurcation.
6. Perfuse the aortic graft with 125 U/mL heparin solution by using a 2 mL disposable syringe with a 26 G hypodermic needle to wash the vessel clear of all blood components. Store the graft at 4 °C before use.
7. Euthanize the donor rat by cervical dislocation.
8. Take a healthy rat as the recipient. Follow step 2.1 to administer anesthesia, step 2.2 for skin prepping, and steps 3.3 and 3.4 to expose and separate the abdominal aorta.
9. Temporarily block the blood flow of the aorta by inserting two microclamps: one right below the renal branch and the other at aortic bifurcation.
10. Transect the abdominal aorta with microscissors at the midpoint of the renal arteries and aortic bifurcation. Rinse the cut ends with heparin solution by using a 2 mL disposable syringe with a 26 G hypodermic needle.
11. Anastomose the graft aorta to the recipient aorta in an end-to-end manner by running stitches with a 9-0 nylon suture. Use a microneedle holder and microtweezers to perform the anastomosis.
12. Remove the microclamps to restore the blood flow.
13. Use one of the following two hemostat methods if anastomotic bleeding occurs.
    1. Simply press the anastomosis with a dry cotton swab for 30 s if the bleeding is not serious.
    2. Apply tissue adhesive to stop the bleeding if it is not easy to control.
        1. Use the microclamps again to stop the bleeding and apply a 0.5 µL aliquot of tissue adhesive along the anastomotic line with a 2 µL pipette.
        2. Wait 10 s to form a strong and transparent layer of hemostat covering around the anastomosis. Take the microclamps away to check the patency and bleeding of the anastomosis.

3. Keep in mind that applying too much adhesive results in anastomotic stenosis and subsequent thrombus formation.

14. Close the abdominal incision by a running 3-0 polyglactin suture.
15. Keep the recipient in a warming blanket until it has recovered from the anesthesia.
16. Inject 1 mL of normal saline *via* the tail vein if blood loss is estimated to exceed 2 mL.
17. Feed the recipient on water and a normal diet after the operation.
18. Euthanize the recipient on postoperative day 90 to procure the graft aorta for biomedical analysis. Please note that the vascular anastomoses are carefully removed to avoid the effect of suture material on the evaluation of the vasculopathy.

## 4. MSC Infusion

1. Label MSCs with green fluorescence protein (GFP) by viral transfection, according to the a previous report[15]. Analyze the expression of MSC markers (positive for CD90, CD44, and CD29, and negative for CD34, CD45, and CD11b/c) to make it sure that there are no significant changes after the viral transfection (**Table 2**).
2. Prepare fresh MSCs in serum-free medium. Follow step 2.1 to anesthetize the rats for the MSC infusion.
3. Infuse MSCs *via* tail vein to each rat at a dose of 2 x $10^6$ cells for 4x, starting from the 30th day after the irradiation with an interval of 15 days. Keep the infused rat in a warming blanket until it has recovered from the anesthesia.

## 5. Histology Analysis

1. Fix fresh aortic specimens in 10% formalin for 12 h. Rinse the tissue with phosphate-buffered solution (PBS) until the formalin is completely removed.
2. Dehydrate the aortic tissue in the automated vacuum tissue processor. Embed the tissue in fresh new paraffin and cut it into 5 µm cross sections.
3. Stain the sections with hematoxylin-eosin and Masson's trichrome to evaluate the vasculopathy.
4. Stain the sections by the standard avidin-biotin complex technique to measure the expression of myeloperoxidase (MPO) 16.
5. Obtain slide images under a digital slide scanner. Measure the thickness of the vascular wall by slide image analysis software. Normalize the intimal thickness to the full thickness of the vascular wall to obtain the relative value.

## 6. Fluorescent Staining

1. Mount fresh graft aorta in OCT compound and cut it into 5 µm cross sections.
2. Stain the nuclei with 4′,6-diamidino-2-phenylindole (DAPI).
   CAUTION: DAPI is mutagenic, and it should be handled with precaution.
3. Count GFP-labeled cells in the sections under a fluorescent microscope.
4. Calculate the average number of GFP-labeled cells per high-power field (HPF) from three random HPFs for each rat. Investigate eight rats from each group to obtain the average.

## 7. Real-time Quantitative Reverse Transcription Polymerase Chain Reaction

1. **Total RNA extraction**
   1. Store fresh graft aorta tissue in liquid nitrogen immediately after it is harvested.
   2. Weigh 5 mg of the aortic sample from each rat. Put the eight samples of the same group together as a biopsy specimen of 40 mg from the group. Homogenize the aortic tissue with a Dounce tissue grinder in an ice bath.
   3. Add 1 mL of commercial trypsin solution to dissolve the tissue fragment and transfer the homogenate to a 2 mL centrifuge tube for centrifugation at 12,000 x *g* for 10 min at 4 °C.
   4. Transfer the supernatant to a prechilled, fresh 2 mL centrifuge tube and keep it at room temperature for 5 min.
   5. Add 0.2 mL of chloroform, vortex for 15 s, and leave it at room temperature for 3 min. Centrifuge at 12,000 x *g* for 15 min at 4 °C.
   6. Transfer the aqueous phase (the top phase) to a fresh 2 mL centrifuge tube, being careful not to contaminate the solution with the other phases. Add 0.5 mL of isopropanol, mix them together, and incubate at room temperature for 10 min.
   7. Centrifuge at 12,000 x *g* for 10 min at 4 °C. Discard the supernatant, wash the RNA pellet with 1 mL of 75% EtOH, and vortex for 15 s.
   8. Centrifuge at 7,500 x *g* for 5 min at 4 °C. Remove the supernatant and allow the remaining EtOH to air-dry for 3 min.
   9. Dissolve the RNA pellet in 20 µL of diethylpyrocarbonate-treated water and store it at -70 °C.

2. **Reverse transcription**
   1. Prepare 10 µL of reaction mixture for each reaction. Mount each microtube with 2 µL of 5x Polymerase Master Mix, 2 µL of 100 ng/µL total RNA solution, and 6 µL of ultrapure water, as required to reach 10 µL.
   2. Place the microtubes in a polymerase chain reaction (PCR) system. Start to run the program settings: 15 min at 37 °C, followed by 5 s at 85 °C.
   3. Store the microtubes in an ice bath.

3. **PCR analysis for cDNA samples**
   1. Prepare the primers of the following cytokines for cDNA template, according to previous studies[17,18]: tumor necrosis factor α (TNFα) forward primer 5'-CACGCTCTTCTGTCTACTGA-3' and reverse primer 5'-GGACTCCGTGATGTCTAAGT-3'; transforming growth factor β (TGFβ) forward primer 5'-CCTGGGCACCATCCATGA-3' and reverse primer 5'-CAGGTGTTGAGCCCTTTCCA-3'; interleukin 1β (IL-1β) forward primer 5'-GGGTTGAATCTATACCTGTCCTGTGT-3' and reverse primer 5'-GACAAACCGCTTTTCCATCTTCT-3'; interleukin 2 (IL-2) forward primer 5'-CAGCTCGCATCCTGTGTTGCAC-3'and reverse primer 3'-GCTTTGACAGATGGCTATCCATC-3'.

2. Prepare 20 µL of reaction mixture for each reaction. Mount each microtube with 10 µL of 2x SYBR Premix Ex Taq II, 0.8 µL of forward primer, 0.8 µL of reverse primer, 0.4 µL of 50x ROX Reference Dye, 2 µL of cDNA solution, and 6 µL of ultrapure water, as required to reach 20 µL.
3. Place the microtubes in the PCR system. Start to run the program settings: 30 s at 95 °C, followed by 40 cycles of 5 s at 95 °C and 30 s at 60 °C.
4. Calculate the target RNA expression of each group by being normalized to that of β-actin and vehicle control using the comparative cycle threshold method.

## 8. Real-time Quantitative PCR

1. **Genomic DNA preparation**
   1. Mount a fresh tube with a biopsy specimen of 10 mg from each group. Add lysis buffer A and proteinase K solution at 180 µL and 20 µL, respectively, vortex for 15 s, and incubate at 55 °C for 3 h to dissolve the tissue.
   2. Add 200 µL of lysis buffer B, vortex for 15 s, and incubate at 70 °C for 10 min.
   3. Add 200 µL of anhydrous ethanol and vortex for 15 s. Load the above mixture to a DNA purification column and centrifuge at 6,000 x *g* for 1 min.
   4. Wash the column with 500 µL of buffer I and centrifuge at 6,000 x *g* for 1 min. Wash the column with 600 µL of buffer II and centrifuge at 18,000 x *g* for 2 min.
   5. Load 200 µL of elution buffer to the column, keep it still at room temperature for 3 min, and centrifuge at 18,000 x *g* for 1 min. Place a fresh tube under the column to collect all elution which contains purified DNA.

2. **PCR analysis for DNA samples**
   1. Prepare the primers for the Sry gene and for the housekeeping gene β-actin according to the reported sequence[19]: Sry forward primer 5'-GAGGCACAAGTTGGCTCAACA-3' and reverse primer 5'-CTCCTGCAAAAAGGGCCTTT-3'; β-actin forward primer 5'-CCATTGAACACGGCATTG-3' and reverse primer 5'-TACGACCAGAGGCATACA-3'.
   2. Prepare 20 µL of reaction mixture for each reaction. Mount each microtube with 10 µL of 2x SYBR Green qPCR Master Mix, 1 µL of forward primer, 1 µL of reverse primer, 2 µL of 50 ng/µL DNA template, and 6 µL of ultrapure water, as required to reach 20 µL.
   3. Place the microtubes in the PCR system. Use the PCR program settings: 30 s at 95 °C, followed by 40 cycles of 5 s at 95 °C and 30 s at 60 °C.
   4. Calculate the Sry DNA levels by being normalized to that of β-actin using the comparative cycle threshold method.

## 9. Statistical Analysis

1. Express the data as the mean ± standard deviation. Make a group comparison by using the Mann–Whitney test. Consider a *p*-value of <0.05 to indicate statistical significance.

## Representative Results

On postoperative day 90, the segment of irradiated graft aorta was procured for histological analysis. The vascular injury consisted of intimal hyperplasia and vascular fibrosis, which resembled the histological changes of irradiated vessels reported previously[4]. The hyperplastic intima was formed by an accumulation of abundant spindle-shaped cells and extracellular matrix mixed with some degree of inflammatory cell infiltration. In Masson's trichrome stain, the amount of blue-stained collagen fiber was increased in all layers of the irradiated aorta, suggesting diffuse vascular fibrosis after irradiation. Moreover, a large number of MPO-positive cells gathered in the adventitia of the irradiated aorta. This indicated that severe oxidative stress occurred as it is commonly present in radiation injury[20]. In comparison, the histological response was almost the same between the RT-plus-TX and RT-only groups, while the aorta remained almost normal in the TX-only group as compared to the vehicle control. However, the groups with MSC treatment (the RT-plus-TX + MSC and RT-only + MSC groups) demonstrated a great histological relief when compared with the RT-plus-TX and RT-only groups. The thickness of intima was significantly decreased, and diffuse fibrosis and inflammatory cell infiltration were also attenuated (**Figure 1**). Notably, MSC infusion had a more favorable effect on intimal hyperplasia in the RT-plus-TX model than in the RT-only model since the RT-plus-TX + MSC group had a significantly lower average thickness of intima (**Figure 2**).

Next, the homogenate of the irradiated aorta was sent for PCR analysis of inflammatory cytokines, including TNF-α, TGF-β, IL-1β, and IL-2. All cytokines were significantly increased in both RT-plus-TX and RT-only groups as compared to the TX-only and vehicle control groups (**Figure 3**). This suggested a proinflammatory response to radiation injury, which is consistent with previous studies[20,21]. However, MSC infusion attenuated vascular inflammation since most of these cytokine levels were significantly decreased in the groups with MSC treatment. Notably, the RT-plus-TX + MSC group had a greater decrease of TGF-β level than the RT-only + MSC group.

Last, the homing of MSCs to the irradiated aorta was assessed by counting GFP-labeled cells under a fluorescent microscope. GFP-labeled cells were preferably engrafted into the intima layer at the average density of 3.30 cells/HPF in the RT-plus-TX + MSC group. In contrast, GFP-labeled cells were nearly invisible in the RT-only + MSC group. The result was supported by PCR analysis for the Sry gene. The RT-plus-TX + MSC group had a significantly higher level of Sry gene than the RT-only + MSC group (**Figure 4**). Therefore, the homing of MSCs to the irradiated aorta was greatly improved by utilizing the RT-plus-TX model.

| Group | n | Radiation | Aorta Transplantation | MSC infusion |
|---|---|---|---|---|
| Vehicle control | 8 | - | - | - |
| RT-only | 8 | + | - | - |
| TX-only | 8 | - | + | - |
| RT-plus-TX | 8 | + | + | - |
| RT-only+MSC | 8 | + | - | + |
| RT-plus-TX+MSC | 8 | + | + | + |

**Table 1: Animal groups and treatment protocols.** The symbols of '+' and '-' represent whether the referred treatment was given or not, respectively.

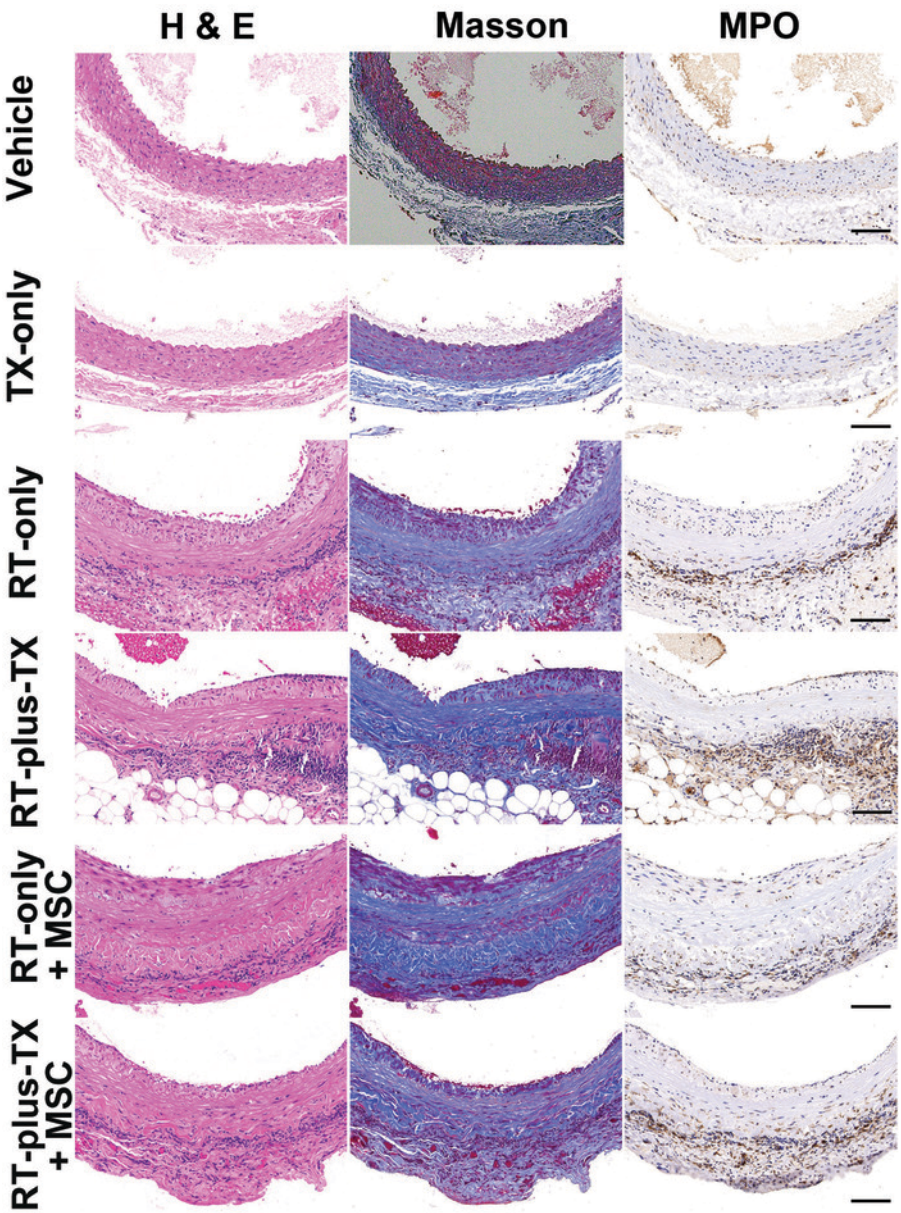


**Figure 1: Cross-sectional images of the abdominal aorta.** Serial cross sections of the aorta were processed with hematoxylin-eosin stain (H&E), Masson's trichrome stain (Masson), or immunostain with antimyeloperoxidase antibody using a DAB substrate kit (MPO). The images represent the investigation of eight rats for each group. The scale bar = 100 μm. Please click here to view a larger version of this figure.

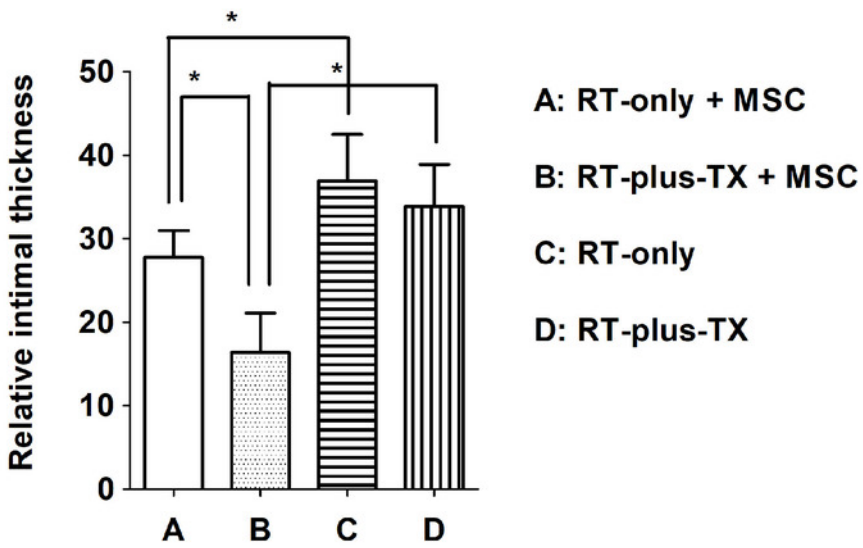


**Figure 2: Histological analysis of intimal hyperplasia.** The relative intimal thickness was normalized to the full thickness of the vascular wall and expressed as a percentage. Eight rats were investigated for each group. Group comparison was performed with the Mann-Whitney test. * $p < 0.05$. The error bar = standard deviation. Please click here to view a larger version of this figure.

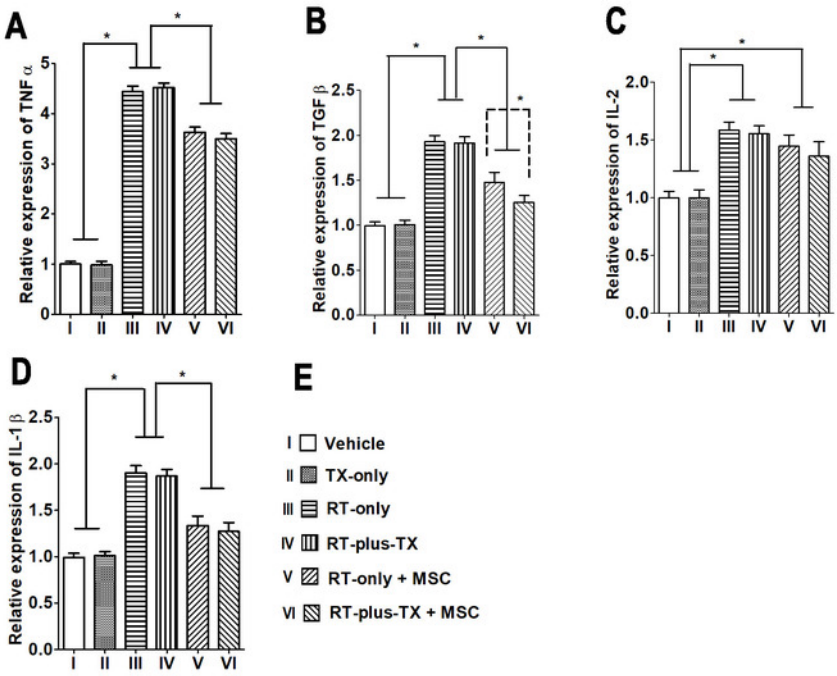


**Figure 3: Expression of proinflammatory cytokines in the aorta.** The expression of (**A**) TNFα, (**B**) TGF β, (**C**) IL-2, and (**D**) IL-1β in study groups is illustrated. The cytokine levels were measured by real-time qualitative reverse transcription PCR and normalized to the vehicle control. The experiment was repeated three times for each group. (**E**) To which one of the study groups each bar referred to in the histogram is indicated. The group comparison was performed with the Mann-Whitney test. * $p < 0.05$. The error bar = standard deviation. Please click here to view a larger version of this figure.

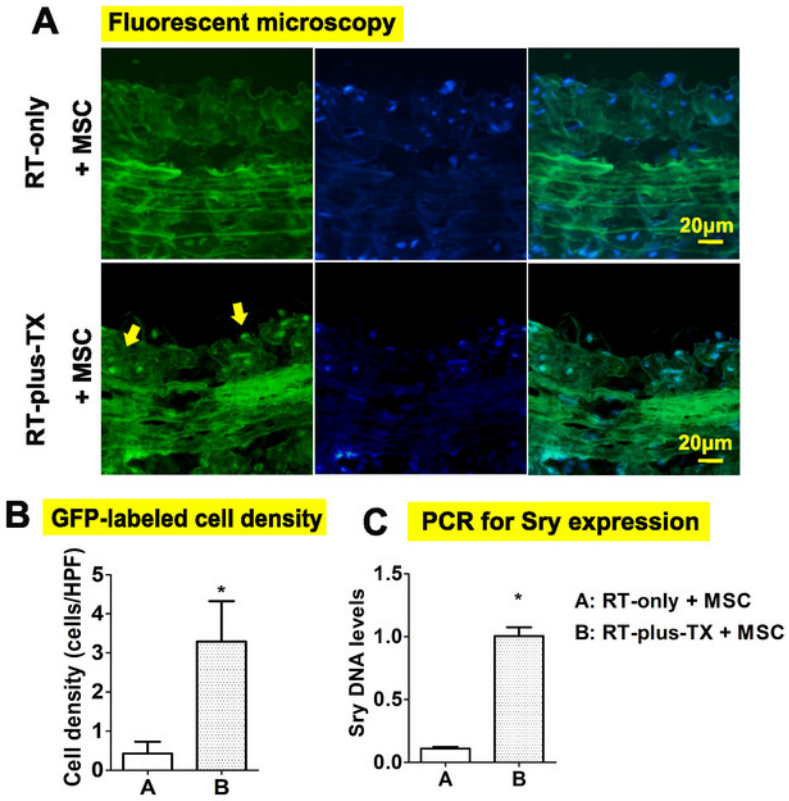


**Figure 4: Migration of mesenchymal stem cells (MSCs) to the irradiated aorta.** MSC migration was investigated by two techniques: fluorescent microscopy for tracing cells with a green fluorescent protein (GFP) label and PCR analysis for the sex determination region on the Y chromosome (Sry) specifically carried by transplanted MSCs. (**A**) The GFP-labelled cells were more frequently present in the intima of the RT-plus-TX model. The density of the GFP-labelled cells was expressed in the cell number per high-power field to quantify the MSC distribution in the irradiated aorta. (**B**) The RT-plus-TX model had a significant increase of GFP-labelled cell density when compared to the RT-only model. (**C**) The Sry level was approximately six-fold higher in the RT-plus-TX model than in the RT-only model. For each group, eight rats were investigated by fluorescent microscopy, and the PCR analysis was repeated three times. The group comparison was performed with the Mann-Whitney test. * $p < 0.05$. The error bar = standard deviation. The scale bar = 20 μm. Please click here to view a larger version of this figure.

## Discussion

The MSC-based therapy holds great promise for treatment of radiation injury. Many animal experiments have demonstrated that the transplantation of MSCs attenuated radiation injury by inhibiting inflammatory response and promoting tissue regeneration[12,22,23]. The homing of MSCs to injured tissue is the prerequisite for generating that effect[13]. However, only a few studies clearly have shown how many cells finally migrate and engraft into irradiated tissues[19,24]. Moreover, highly sensitive methods like PCR analysis for specific biomarkers of transplanted MSCs are preferred to quantify the MSC recruitment in many researches[14,19,24]. This suggests a very low population of homed MSCs like what was revealed in the RT-only model. In this model, the transplanted MSCs with GFP label were seldom present in the irradiated aorta. Although the poor engraftment of MSCs would be multifactorial, the animal model was intrinsically relevant. Despite the use of a beam-limiting device to avoid unnecessary tissue irradiation, the body area that was eventually irradiated not only included the abdominal aorta but also adjacent tissue, both of which were likely to release a damage signal to stimulate MSC migration[25,26,27,28]. Thus, circulating MSCs would also be distributed into the adjacent tissue, which was unintentionally subjected to radiation injury, yet form a larger compartment of MSC homing than the irradiated aorta alone. In that case, the fraction of MSCs recruited to the irradiated aorta would be greatly decreased. Conversely, if the aorta was exclusively subjected to radiation injury, more circulating MSCs would gather in the irradiated aorta. The theory is supported by an early study which found that local irradiation promotes the migration of MSCs to the irradiated field[14]. Therefore, this study introduced the RT-plus-TX model. In this model, the aorta of the irradiated rat was anatomically separated from adjacent tissue and transplanted to the healthy counterpart. Although the irradiated vascular graft developed almost the same histological changes as what was seen in the RT-only model, a significant increase of transplanted MSCs with GFP label and Sry gene was found in the vascular graft. The following calculation predicted the relative changes of the MSC density in the irradiated aorta after the separation of the aorta from adjacent tissue like in the RT-plus-TX model.

In the RT-only model, the volume of irradiated tissue ($V_{RT\text{-}only}$) was calculated by multiplying the length (L), width (W), and depth (D) of the body compartment exposed to radiation. The length and width were determined by the square-shaped irradiation field of 3 x 3 cm, and the depth was the thickness of the rat posterior abdominal wall, approximately 1.5 cm on average. The result is shown as follows.

$V_{RT\text{-}only}$ = 3 cm (*L*) × 3cm(*W*) × 1.5 cm(*D*) = 13.5 $cm^3$

In the RT-plus-TX model, the aortic graft was the only tissue with irradiation. The graft was shaped like a cylinder with a height (H) of 1.5 cm and a cycle base area of 1 mm in diameter (A). The formula to calculate the irradiated volume ($V_{RT\text{-}plus\text{-}TX}$) is shown as follows.

$V_{RT\text{-}plus\text{-}TX}$ = 1.5 cm (*H*) × π × (0.1 cm (*A*)/2)$^2$= 0.012 cm$^3$

If migrating MSCs are evenly distributed in the irradiated tissue, and if the number of migrating MSCs is constant (*i.e.*, the sum of infused MSCs possessing the high capacity of migration is not different between the RT-only + MSC and RT-plus-TX + MSC groups), then the MSC density of irradiated tissue is inversely proportional to the volume of irradiated tissue. Therefore, the MSC density (DEN) was calculated from the following formula.

$DEN_{RT\text{-}plus\text{-}TX}$ / $DEN_{RT\text{-}only}$ = $V_{RT\text{-}only}$ / $V_{RT\text{-}plus\text{-}TX}$ = 13.5 cm$^3$/ 0.0118 cm$^3$= 1.14 x 10$^3$

As a result, the irradiated aortas of the RT-plus-TX+ MSC group were estimated to have approximately a 1,000x higher MSC density than those of the RT-only+ MSC group. In that case, the density of GFP-labeled cells in the RT-only + MSC group was anticipated to be 0.0029 (3.30 / 1.14 x 10$^3$) cells/HPF, which suggested a fairly low incidence of detecting GFP-labeled cells under fluorescent microscopy. The estimate was supportive of what was observed in this experiment, although many factors, like whether migrating MSCs were evenly distributed between the aorta and adjacent tissue, were neglected. Intriguingly, a previous study revealed that MSCs were preferably homed to the viscera, skin, and muscle, but not aorta, after local irradiation[14]. In other words, the aorta was not the favorable destination for MSCs as compared to adjacent tissue and organs if isodose irradiation was given. Therefore, the sequestration of the irradiated aorta was presumably helpful to diminish the preference of MSC recruitment to adjacent tissue. Generally, the RT-plus-TX model supported the theory that simultaneously irradiated adjacent tissue interfered with the gathering of MSCs to the irradiated aorta. The sequestration of irradiated rat aorta by transplantation to a healthy counterpart was an effective way to improve the MSC local recruitment.

However, the RT-plus-TX model had some drawbacks. First, this model is suitable for the study of large vessels but not the microvascular system. Radiation vasculitis is morphologically different depending on the size of the vessels. When compared with large vessels, capillary vessels are prone to rupture and dilate and form thrombus after irradiation[29]. Such pathological features were not present in the RT-plus-TX model. Moreover, the method to sequester irradiated vessels as described in this model is not applicable to microvasculature, since the transplantation of capillary vessels alone is technically difficult. Second, the RT-plus-TX model is not easy to use, especially for beginners who have had no training for microsurgery. The major obstacle is to complete aortic anastomosis in a short time without any serious complication like bleeding and thrombosis. Therefore, the technique of cyanoacrylate-assisted vascular anastomosis was introduced to simplify the procedure of aorta transplantation and improve the success rate. The use of cyanoacrylate is safe and effective enough, as reported in many studies[30,31,32]. Third, some might argue that the RT-plus-TX model is not reliable because surgical trauma, such as ischemia-reperfusion injury, will accelerate the progression of radiation vasculitis. Admittedly, surgical trauma is unavoidable in this model, given that aorta transplantation is indispensable to sequester irradiated aorta. But most follow-up effects of surgical trauma were temporary, being initiated shortly after the operation and regressing within 1 month according to a previous study[32]. Moreover, the interference of surgical trauma was well controlled by setting up the RT-only group which served as sham surgery control. Consequently, the RT-plus-TX group shared similar pathological features of radiation vasculitis as the RT-only group. Last, the contribution of immune rejection was eliminated by the transplantation between F344 inbred rats which possessed minimal genetic differences within the strain.

Generally, the RT-plus-TX model promotes MSC accumulation in irradiated vessels by separating an irradiated vascular segment from adjacent tissue. This model is preferred in the study of MSC-based therapy for radiation vasculitis when the evaluation of MSC homing is demanding.

## Disclosures

The authors have nothing to disclose.

## Acknowledgements

This study was made possible by grants from the National Natural Science Foundation of China (81400306), the Project of Medicine and Health Science and Technology of Zhejiang Province (2014KYA175), and the Project of Invigorating Health Care through Science, Technology and Education of Jiangsu Province Medical Youth Talent (QNRC2016671).

## References

1. Chen, J. H. *et al.* Dementia Risk in Irradiated Patients With Head and Neck Cancer. *Medicine (Baltimore).* **94**(45), e1983 (2015).
2. Tang, Y., Luo, D., Rong, X., Shi, X., Peng, Y. Psychological disorders, cognitive dysfunction and quality of life in nasopharyngeal carcinoma patients with radiation-induced brain injury. *PLoS One.* **7**(6), e36529 (2012).
3. Chong, V. F., Khoo, J. B., Chan, L. L., Rumpel, H. Neurological changes following radiation therapy for head and neck tumours. *European Journal of Radiology.* **44**(2), 120-129 (2002).
4. Xu, J., Cao, Y. Radiation-induced carotid artery stenosis: a comprehensive review of the literature. *Interventional Neurology.* **2**(4), 183-192 (2014).
5. Harb, A. H., Abou Fadel, C., Sharara, A. I. Radiation enteritis. *Current Gastroenterology Report.* **16**(5), 383 (2014).
6. Doi, H. *et al.* Long-term sequential changes of radiation proctitis and angiopathy in rats. *Journal of Radiation Research.* **53**(2), 217-224 (2012).
7. Gurses, I., Ozeren, M., Serin, M., Yucel, N., Erkal, H. S. Histopathological efficiency of amifostine in radiationinduced heart disease in rats. *Bratislavské Lekárske Listy.* **119**(1), 54-59 (2018).
8. Gu, W., Hong, X., Potter, C., Qu, A., Xu, Q. Mesenchymal stem cells and vascular regeneration. *Microcirculation.* **24**(1) (2017).

 

9. Zaher, W., Harkness, L., Jafari, A., Kassem, M. An update of human mesenchymal stem cell biology and their clinical uses. *Archives of Toxicology.* **88**(5), 1069-1082 (2014).
10. Molthen, R. C. *et al.* Mitigation of radiation induced pulmonary vascular injury by delayed treatment with captopril. *Respirology.* **17**(8), 1261-1268 (2012).
11. Stewart, F. A. *et al.* Ionizing radiation accelerates the development of atherosclerotic lesions in ApoE-/- mice and predisposes to an inflammatory plaque phenotype prone to hemorrhage. *American Journal of Pathology.* **168**(2), 649-658 (2006).
12. Shen, Y. *et al.* Transplantation of Bone Marrow Mesenchymal Stem Cells Prevents Radiation-Induced Artery Injury by Suppressing Oxidative Stress and Inflammation. *Oxidative Medicine and Cellular Longevity.* **2018**, 5942916 (2018).
13. Mouiseddine, M. *et al.* Human mesenchymal stem cells home specifically to radiation-injured tissues in a non-obese diabetes/severe combined immunodeficiency mouse model. *British Journal of Radiology.* **80 Spec No 1**, S49-55 (2007).
14. Francois, S. *et al.* Local irradiation not only induces homing of human mesenchymal stem cells at exposed sites but promotes their widespread engraftment to multiple organs: a study of their quantitative distribution after irradiation damage. *Stem Cells.* **24**(4), 1020-1029 (2006).
15. Meng, X. *et al.* The differentiation of mesenchymal stem cells to vascular cells regulated by the HMGB1/RAGE axis: its application in cell therapy for transplant arteriosclerosis. *Stem Cell Research & Therapy.* **9**(1), 85 (2018).
16. Wang, J., Zheng, H., Ou, X., Fink, L. M., Hauer-Jensen, M. Deficiency of microvascular thrombomodulin and up-regulation of protease-activated receptor-1 in irradiated rat intestine: possible link between endothelial dysfunction and chronic radiation fibrosis. *American Journal of Pathology.* **160**(6), 2063-2072 (2002).
17. Calveley, V. L., Khan, M. A., Yeung, I. W., Vandyk, J., Hill, R. P. Partial volume rat lung irradiation: temporal fluctuations of in-field and out-of-field DNA damage and inflammatory cytokines following irradiation. *International Journal of Radiation Biology.* **81**(12), 887-899 (2005).
18. Zuo, X. J. *et al.* Cytokine gene expression in rejecting and tolerant rat lung allograft models: analysis by RT-PCR. *Transplant Immunology.* **3**(2), 151-161 (1995).
19. Shao, C. H. *et al.* Transplantation of bone marrow-derived mesenchymal stem cells after regional hepatic irradiation ameliorates thioacetamide-induced liver fibrosis in rats. *Journal of Surgical Research.* **186**(1), 408-416 (2014).
20. Zhao, W., Robbins, M. E. Inflammation and chronic oxidative stress in radiation-induced late normal tissue injury: therapeutic implications. *Current Medical Chemistry.* **16**(2), 130-143 (2009).
21. Gallet, P. *et al.* Long-term alterations of cytokines and growth factors expression in irradiated tissues and relation with histological severity scoring. *PLoS One.* **6**(12), e29399 (2011).
22. Chang, P. *et al.* Multi-therapeutic effects of human adipose-derived mesenchymal stem cells on radiation-induced intestinal injury. *Cell Death & Disease.* **4**, e685 (2013).
23. Nicolay, N. H., Lopez Perez, R., Debus, J., Huber, P. E. Mesenchymal stem cells - A new hope for radiotherapy-induced tissue damage? *Cancer Letters.* **366**(2), 133-140 (2015).
24. Yang, D. *et al.* Stromal cell-derived factor-1 receptor CXCR4-overexpressing bone marrow mesenchymal stem cells accelerate wound healing by migrating into skin injury areas. *Cell Reprogramming.* **15**(3), 206-215 (2013).
25. Mahrouf-Yorgov, M. *et al.* Mesenchymal stem cells sense mitochondria released from damaged cells as danger signals to activate their rescue properties. *Cell Death & Differentiation.* **24**(7), 1224-1238 (2017).
26. Palumbo, R. *et al.* Cells migrating to sites of tissue damage in response to the danger signal HMGB1 require NF-kappaB activation. *Journal of Cell Biology.* **179**(1), 33-40 (2007).
27. Pateras, I. S. *et al.* The DNA damage response and immune signaling alliance: Is it good or bad? Nature decides when and where. *Pharmacological Therapy.* **154**, 36-56 (2015).
28. Stoecklein, V. M. *et al.* Radiation exposure induces inflammasome pathway activation in immune cells. *Journal of Immunology.* **194**(3), 1178-1189 (2015).
29. Fajardo, L. F. The pathology of ionizing radiation as defined by morphologic patterns. *Acta Oncology.* **44**(1), 13-22 (2005).
30. Kim, B. Y. *et al.* Microvascular anastomosis using cyanoacrylate adhesives. *Journal of Reconstructive Microsurgery.* **20**(4), 317-321 (2004).
31. Saba, D. *et al.* Sutureless vascular anastomoses by N-butyl-2 cyanoacrylate adhesive: an experimental animal study. *European Surgical Research.* **39**(4), 239-244 (2007).
32. Wei, W., Zhu, Y., Wang, J., Li, Y., Li, J. Cyanoacrylate-assisted arterial anastomosis in rat small bowel transplantation. *Langenbecks Archives of Surgery.* **395**(6), 727-735 (2010).


 